

Three-dimensional electron diffraction mapping for cyclic twinned nanostructures

Xin Fu¹ and Jun Yuan²

¹ General Research Institute for Nonferrous Metals, Beijing, 100088, P.R. China

² Department of Physics, University of York, York YO10 5DD, United Kingdom

Email: fuxints@gmail.com

Abstract. In recent years, the information retrieval of three-dimensional (3D) intensity distribution in reciprocal space has attracted much attention in nanometrology research. However, the development of 3D analysis of electron diffraction intensity including crystal structural identification and morphology determination of nanocrystals have so far focused on single crystalline nano-objects. Using boron carbide five-fold twinned nanowires as a model system for nanostructured nano-objects, we demonstrated that such method can also identify the internal structure of cyclic twinned nanostructures. Here, the methodology of the 3D mapping of electron diffraction from such nanowires will be presented and the approach is compared with the conventional method of axial rotation electron diffraction analysis to demonstrate its comprehensive, quantitative and non-destructive nature. We believe that such approach can be easily extended to the investigation of internal structures of other polycrystalline nanostructures.

1. Introduction

Cyclic twinned nanostructures, such as five-fold twinned nanoparticles and nanowires, have drawn much research interests due to the unusual internal structure and the unexpected mechanical properties [1-4]. A direct method of characterization for these nanostructures is through cross-sectional observation by transmission electron microscopy (TEM) [2]. However, it typically requires preparation of ultrathin cross-sectional samples either by microtome or focused ion beam (FIB), both of them inevitably introduce sample damage and creating difficulty in identifying the intrinsic structural defects. The real-space electron tomography is non-destructive but suffers from a ‘missing wedge’ problem [5], and it cannot be routinely used to determine the crystallography of the internal structure. Besides the real-space imaging methods, electron diffraction analysis has also been employed to investigate the structural feature of the complex nanostructures. The conventional approach is to acquire a set of high symmetry zone-axis related electron diffraction patterns from some specific orientations [3, 4]. However, there is a wealth of structural information contained in the relative position and intensity of diffraction spots. 3D analysis of electron diffraction intensity distribution aims to fully exploit such information and has been applied in crystal structure identification and morphology determination of nanocrystals, so far all focusing on single crystalline nano-objects [6, 7]. Here, we demonstrated the approach and advantages of the 3D electron diffraction mapping method for revealing the internal structure of cyclic twinned nanostructures and contrast this with the conventional approach using the axial rotation electron diffraction analysis.



2. Axial rotation electron diffraction analysis

For boron-rich five-fold twinned nanowire model system, an ideal structure has been proposed [3, 4]. It consists of five identical crystalline segments sharing a common $[001]_r$ (r refers to the rhombohedral representation of the unit cell) axis along the nanowire growth direction and joined together by $\{100\}_r$ twinned planes. Fig. 1a shows the cross-sectional view where five constituent segments are marked with different colors and identified from T1 to T5 for convenience. To identify this twinning structure experimentally, at least three different characteristic diffraction patterns, 18 degrees apart, must be recorded in the conventional method of axial rotation electron diffraction analysis, as shown in Fig. 1. This is consistent with the five-fold pseudo-symmetry of such nanostructures (Fig. 1a and 1e).

For example, if the nanowire is initially oriented in such a way that a mirror-symmetric diffraction pattern can be obtained as shown in Fig. 1c, then the nanowire can be rotated along its own long axis (RT in Fig.1a) either clockwise or anticlockwise by the angle of 18° , and two additional characteristic diffraction patterns with one of the crystalline segments at a $[1\bar{1}0]_r$ zone-axis orientation should be seen. Comparison with simulated diffraction pattern using the idealized structural model suggests that in this case T2 is oriented along the $[1\bar{1}0]_r$ zone-axis in Fig.1b, and T5 is approximately oriented along the $[1\bar{1}0]_r$ zone-axis in Fig.1d. If the nanowire is oriented such that one segment is already close to the $[1\bar{1}0]_r$ zone-axis, as shown in Fig. 1g which is in the same orientation as that shown in Fig. 1b and Fig. 1d, then the nanowire can be rotated clockwise and anticlockwise by 18° along its long axis to observe two mirror-symmetric diffraction patterns respectively. Because of the rhombohedral structure, further tilting the nanowire by approximate 7° , along the direction perpendicular to its long axis, will be required to reveal the mirror-symmetric diffraction patterns with one segment oriented to $[\bar{1}\bar{1}1]_r$ zone-axis as shown in Fig. 1f and Fig. 1h. As a result, such diffraction analysis is complex when applied to an unknown structure. In addition, the large angle of rotation involved is also practically inconvenient for most analytical TEMs where the tilting ranges of the specimen holders are restricted to $\pm 20^\circ$ or $\pm 30^\circ$ due to the limited space inside the pole piece of the objective lens. If the initial orientation of the nanowires is too far off the orientation as shown in Fig. 1c or Fig. 1g, not all three characteristic diffraction patterns, Fig. 1b-1d or Fig. 1f-1h, may be accessible experimentally. In addition, the diffraction information at a large range of orientations is not effectively used because of their complex and low-symmetry features.

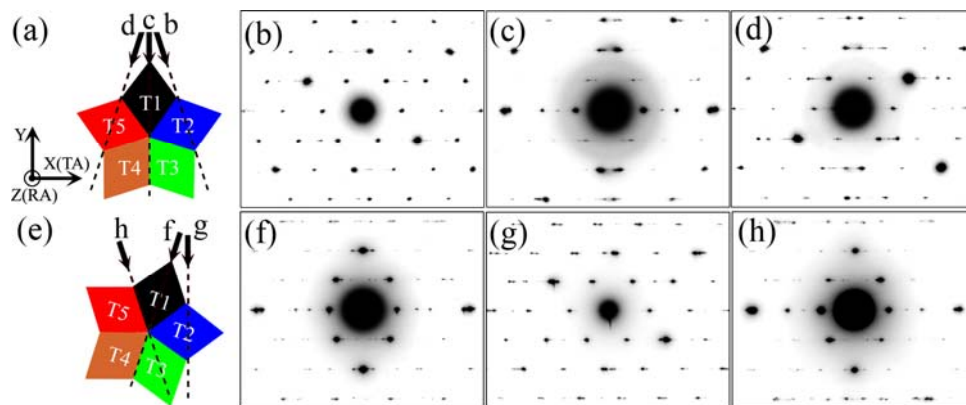


Fig.1 Identification of B₄C five-fold twinned nanowires (five segments are labeled as T1-T5) through electron diffraction analysis under the axial rotation conditions. (a) and (e) illustrate the 18° orientation relationship of the nanowire with the incident electron beam (black arrows) viewed down the nanowire's axis (i.e. the $[001]_r$ direction). The corresponding diffraction patterns shown in (b)-(d) respectively are obtained by successive 18° rotations along the nanowire's axis (RT as shown in (a)). The same approach is used to generate (f)-(h), except that (f) and (h) has been tilted additionally approximate 7° along an axis perpendicular to the nanowire's axis after axial rotation, because of the low symmetry rhombohedral unit cell, to reveal $[\bar{1}\bar{1}1]_r$ zone-axis diffraction from T1 and T3 segments respectively.

3. Three-dimensional (3D) electron diffraction mapping

The essence of 3D electron diffraction mapping is to recreate the 3D intensity distribution of specific reflections in reciprocal space. Experimentally, this is achieved by recording a series of systematic tilting two-dimensional electron diffraction patterns and then using those as the basis for the following 3D reconstruction of the specific reflection.

For the B_4C five-fold twinned nanowire, we start by orienting the nanowire such that the diffraction pattern shown in Fig. 1c is generated and a series of systematic tilting diffraction pattern is collected by either tilting the nanowires or the incident electron beam along the tilting axis (TA, i.e. X axis shown in Fig. 2a), with step of 1° and an overall tilting range about $\pm 10^\circ$. The recorded diffraction patterns share a common feature of a set of diffraction spots along an invariant line (perpendicular to the mirror symmetry plane of the nanowire) which is parallel to the tilting axis (TA) as shown in Fig 2c. The invariant line consists of a systematic row of spots due to diffraction by a set of $(1\bar{1}0)_r$ planes of T1 and a set of $(100)_r$ planes ($(0\bar{1}0)_r$ planes) of T3 (T4) (Fig. 2b). As shown in Fig. 2c, each of the recorded diffraction image represents the intersection of the plane-like segment of the Edward sphere, associated with the 200kV electron beam, with the reciprocal lattice structures of the crystalline components of the nanowires and as such that the raw data of the series of systematic tilting electron diffraction patterns samples the 3D reciprocal space, although with irregularly shaped volume element.

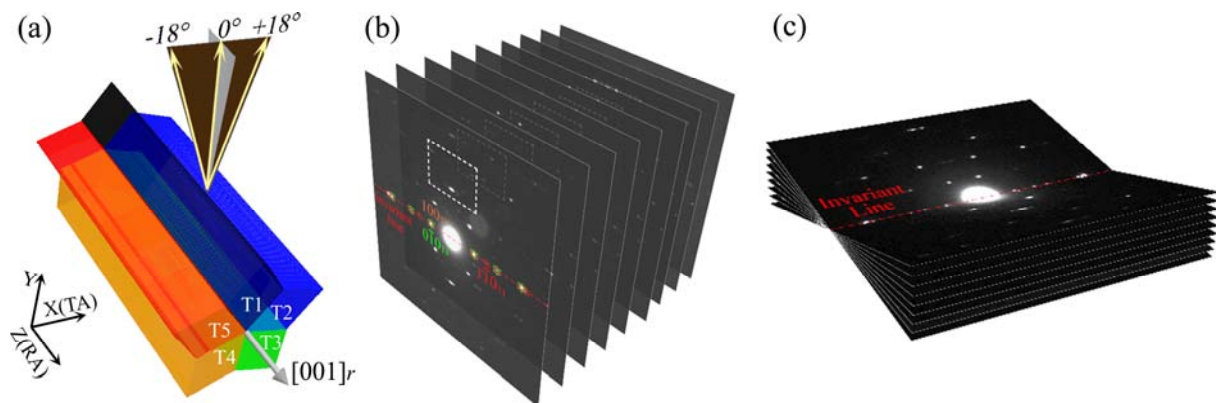


Fig. 2 (a) Schematic view of the orientation relationship between a B_4C five-fold cyclic twinned nanowires and the incident electron beam. The grey plane represents the tilting range of the incident electron beam in the 3D electron diffraction mapping. The arrows in the brown plane indicate the direction of the incident electron beams for the axial rotation electron diffraction. (b) The stack of the collected systematic-tilting diffraction patterns. The dashed rectangle indicates the data extracted area which contains the intensity information of $(112)_r$ and $(113)_r$ reflections. (c) The orientation relationship of the collected diffraction patterns for 3D reconstruction of specific reflections in reciprocal space.

To represent the diffraction intensity properly in the reciprocal volume, we need to convert the experimental raw dataset to a 3D representation in reciprocal space with uniform voxels. The schematics of the post-processing involved are shown in Fig. 3a-3b. We extracted a series of 2D intensity data from a rectangular area with the same pixel size and offset the same distance from the invariant line of every diffraction pattern (Fig.2b). In reciprocal space, the extracted 2D slices form a volume with a sectorial cross section viewing along the invariant line as shown in Fig.3a. We obtained a 3D dataset with uniform voxels as illustrated in Fig.3b through interpolation.

Following this approach, a 3D mapping of diffraction intensity distribution, including the $(112)_r$ and $(113)_r$ reflections of the B_4C five-fold twinned nanowire, has been reconstructed [8]. Fig. 3c presents the reciprocal space volume containing the five $(113)_r$ reflections of the B_4C five-fold twinned nanowire. This intensity distribution directly exhibits the cyclic twinning structure, confirming the overall crystallographic feature of the ideal model. However, detailed analysis [8] shows that the five reflections are not identical in their intensity distribution nor in their angular positions, both reflecting the inhomogeneous distribution of strain and microtwin defects within the

five segments. As the nanowire has not been mechanically strained in this method, we have revealed the inhomogeneous nature of the intact B_4C five-fold twinned nanowire. The quantitative nature of the resulting diffraction intensity distribution also means that similar dataset of sufficient fidelity together with the use of high coherent field emission source also opens up the further possibility of diffractive imaging [7] to reveal the real-space distribution of the internal nanostructures.

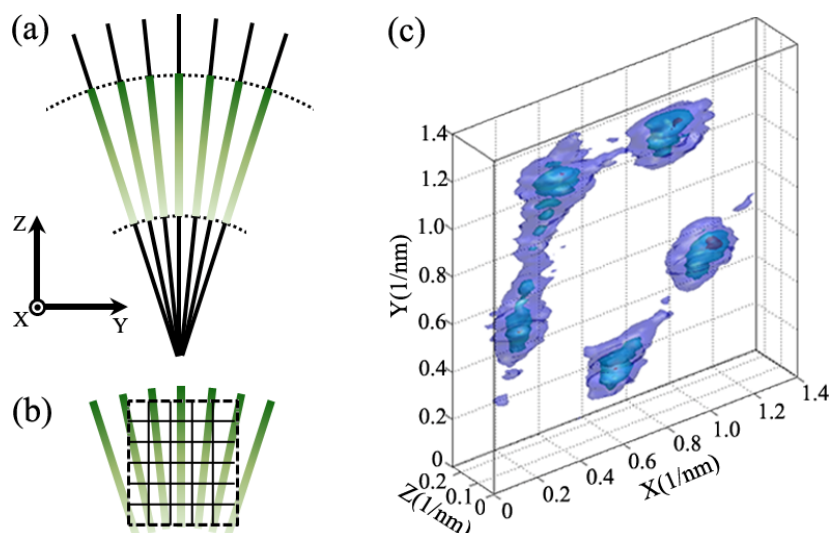


Fig. 3 (a) Schematic view of the tilt series of diffraction patterns aligned along the invariant line (parallel to the X axis, i.e. the tilting axis). The black line with a colored section represents a slice of diffraction pattern. The colored section symbolically indicated the area of interest in the raw data. (b) illustrated the mathematical process applied to raw dataset within the area of interest. (c) The 3D intensity distribution of $(113)_r$ reflections of a B_4C five-fold twinned nanowire.

4. Conclusions

We demonstrated the approach of 3D electron diffraction mapping for cyclic twinned nanostructures. In contrast to the conventional axial rotation electron diffraction analysis, this approach can effectively use the electron diffraction information within a narrow tilting range, so can be used in most analytical microscopes. Additionally, the retrieved quantitative 3D diffraction intensity distribution can provide comprehensive information about the internal structure of such nanocomplex, such as the twinning nature, strain relaxation mechanism and the defect structures.

Acknowledgement

This research is supported by National Natural Science Foundation of China (No. 51201015).

References

- [1] Wu B, Heidelberg A, Boland J J, Sader J E, Sun X M and Li Y D 2006 *Nano Lett.* **6** 468-472
- [2] Chen H Y, Gao Y, Zhang H R, Liu L B, Yu H C, Tian H F, Xie S S and Li J Q 2004 *J. Phys. Chem. B* **108** 12038-12043
- [3] Jiang J, Cao M H, Sun Y K and Yuan J 2006 *Appl. Phys. Lett.* **88** 163107
- [4] Fu X, Jiang J, Liu C and Yuan J 2009 *Nanotechnology* **20** 365707
- [5] Midgley P A and Dunin-Borkowski R E 2009 *Nat. Mater.* **8** 271-280
- [6] Mugnaioli E, Gorelik T and Kolb U 2009 *Ultramicroscopy* **109** 758-765
- [7] Dronyak R, Liang K S, Tstai J-S, Stetsko Y P, Lee T-K and Chen F-R 2010 *Appl. Phys. Lett.* **96** 221907
- [8] Fu X and Yuan J 2013 *Nanoscale* first published online DOI:10.1039/c3nr01839c